RAA 2021 Vol. **21** No. **2**, 44(4pp) doi: 10.1088/1674-4527/21/2/44

http://www.raa-journal.org *http://iopscience.iop.org/raa*

Research in Astronomy and Astrophysics

New observations and transit solutions of the inflated exoplanets HAT-P-40b and HAT-P-51b

Diana P. Kjurkchieva[1], Nikola I. Petrov[2] and Velimir A. Popov[1]

[1] Department of Physics and Astronomy, Shumen University, 115 Universitetska str., 9700 Shumen, Bulgaria; *velimir.popov@elateobservatory.com*

[2] Institute of Astronomy and NAO, Bulgarian Academy of Sciences, Tsarigradsko shossee 72, 1784 Sofia, Bulgaria; *nip.sob@gmail.com*

Received 2020 January 10; accepted 2020 February 28

Abstract We present high-precision photometric observations of the transiting exoplanets HAT-P-40b and HAT-P-51b by the Rozhen 2-m telescope. The newly-observed transit of HAT-P-40b is the first one with a complete curve. The orbital periods of the two targets were improved. We modeled the observed transits and found bigger stellar radii than those derived from the stellar models. The planet radii of HAT-P-40b and HAT-P-51b obtained from our transit solutions are bigger than the values calculated by the empirical relations for Jupiter-mass and Saturn-mass planets respectively. Their values reveal the highly-inflated nature of the two targets, especially that of HAT-P-51b. We established that the best transit solutions correspond to a quadratic limb-darkening law. The fitted limb-darkening coefficients of HAT-P-40 are close to the theoretical ones while those of HAT-P-51 are a little different. The precise astrometric *Gaia* distances of the two targets are smaller by 6%–7% than the calculated values from the stellar models. We propose the *Gaia* distances to be used for improvement of the stellar models as well as for more reliable calculation of the parameters of the known exoplanets.

Key words: (Stars:) planetary systems; techniques: photometric; Stars: individual (HAT-P-40 and HAT-P-51)

1 INTRODUCTION

Transiting extrasolar planets (TEPs) provide a possibility to determine their orbits, physical properties and internal structure.

Statistics reveal that the majority of TEPs have close orbits ($a < 0.1$ AU). Their circularity was attributed to tidal interaction (Goldreich & Soter 1966; Mazeh 2008; Pont et al. 2011).

Many of the known TEPs are giant planets, larger in size than the theoretical predictions (Mandushev et al. 2007; Hebb et al. 2009; Latham et al. 2010; Enoch et al. 2011; Smalley et al. 2012). It was found that the degree of planet inflation depends on their temperatures and orbital axes (Guillot 2005; Enoch et al. 2012).

In this paper we present the results from study of two inflated exoplanets.

2 THE TARGETS

The HATNet survey identified around 2000 exoplanet candidates and 67 were confirmed by spectroscopy. We chose to observe two of them, HAT-P-40b and HAT-P-51b, which have published data only from their discovery papers (Hartman et al. 2012, 2015).

The main goals of our observations were to improve the parameters and ephemerides of the two targets.

2.1 HAT-P-40b

HAT-P-40b was identified as a candidate TEP based on observations made with the HATNet wide-field photometric instruments during 2004–2005 (Hartman et al. 2012). It transits the F9V ($V = 11.7$ mag) star GSC 3607–01028 with an orbital period of $\sim$4.572 d. The follow-up photometric observations in Sloan i filter were obtained with the FLWO, FTN and BOS telescopes in 2010–2011. The spectroscopic observations revealed a radial velocity curve (RVC) with semi-amplitude of 58.1 m s^{-1}.

Hartman et al. (2012) fitted the transit curves and RVC to derive period and initial epoch, orbital inclination, and relative stellar and relative planet radii (in units of planet orbital axis). The authors apply a Mandel & Agol (2002) model with fixed quadratic limb-darkening coefficients.

Table 1 Parameters of HAT-P-40

Parameter	Hartman et al. (2012)	Our solution
P	4.457243(10)	4.457223
T_0	5813.17584(54)	5813.17584*
a	0.0608(11)	0.0608*
i	88.3(9)	86.6(1)
$T_{\rm st}$	6080(100)	6080*
$M_{\rm st}$	1.512(60)	1.512*
$R_{\rm st}$	2.206(61)	2.248(4)
d (pc)	501(16)	464.5(4)*
LDL	quadr	quadr
LDC	0.219*, 0.365*	0.31, 0.363
M_p	0.615(38)	0.615*
R_p	1.730(62)	1.6761(7)
ρ_p	0.15(1)	0.165(2)
T_p	1770(33)*	1000–2600
Θ	0.0286(2)	0.0295(2)

* means fixed parameter.

Table 2 Parameters of HAT-P-51

Parameter	Hartman et al. (2015)	Our Solution
P	4.2180278(59)	4.2180022(1)
T_0	6194.12204(40)	6194.12204*
a	0.05069(49)	0.05069*
i	88.48(0.57)	87.4(1)
$T_{\rm st}$	5450(50)	5450*
$M_{\rm st}$	0.976(28)	0.976*
$R_{\rm st}$	1.041(32)	1.090(1)
d (pc)	470(16)	440(4)*
LDL	quadr	quadr
LDC	0.335*, 0.2989*	0.24, 0.28
M_p	0.309(18)	0.309*
R_p	1.293(54)	1.414(1)
ρ_p	0.178(24)	0.138(1)
T_p	1192(21)*	200–1600
Θ	0.0247(18)	0.0227(5)

The physical parameters of the star HAT-P-40, mass, radius, luminosity and distance, have been determined from a theoretical stellar model on the basis of its effective temperature and metallicity. Then the mass ratio and in turn the planet orbital axis are determined from the mass function. After that, the planet mass and radius are calculated.

Table 1 (column 2) reveals the obtained parameters by Hartman et al. (2012): period P (d); epoch T_0 of transit center (HJD 2450000+); orbital semi-major axis a (AU); orbital inclination i (deg); stellar temperature $T_{\rm st}$ (K); stellar mass $M_{\rm st}$ $(M_\odot)$; stellar radius $R_{\rm st}$ $(R_\odot)$; distance d (pc); limb-darkening law (LDL); limb-darkening coefficients (LDC); planet mass M_p (M_J); planet radius R_p (R_J); planet density ρ_p (g cm^{-3}); planet temperature T_p (K); and Safronov number Θ.

Hartman et al. (2012) concluded that HAT-P-40b falls in the population of large radius ($R > 1.5\,R_J$), sub-Jupiter-mass planets, which are referred to as highly inflated planets.

2.2 HAT-P-51b

HAT-P-51b was identified as a candidate TEP based on HATNet observations during 2008–2011. It transits the G0V ($V = 13.4$ mag) star GSC 2296–00637 with an orbital period of ~ 4.218 d. The follow-up photometric observations in Sloan i filter were obtained with the FLWO telescope in 2012. The spectroscopic observations revealed RVC with semi-amplitude of 40 m s^{-1}.

Following the same procedure as for HAT-P-40, Hartman et al. (2015) obtained the parameter values given in Table 2 (second column). As a result, they classified HAT-P-51b as a hot Saturn-like planet that falls near the upper envelope of the distribution of points in the mass-radius diagram for transiting planets with 0.1 $M_J < M <$ 10 M_J.

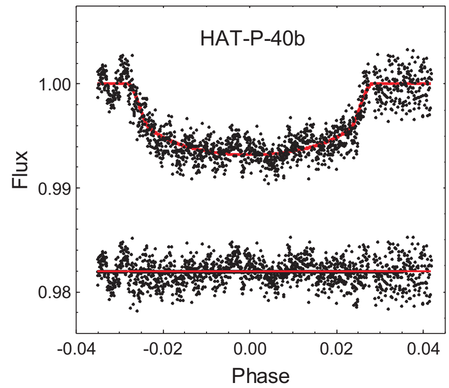

Fig. 1 *Top*: the Rozhen transit of HAT-P-40b and the synthetic curve corresponding to the best solution; *Bottom*: the residuals of the fit.

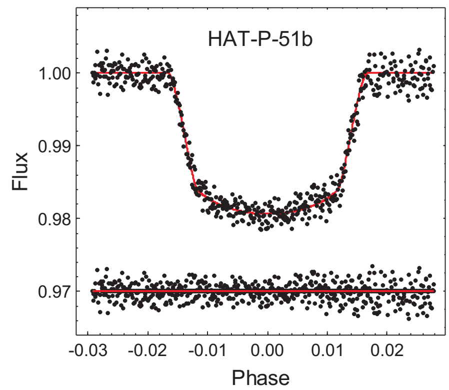

Fig. 2 The same as Fig. 1 for HAT-P-51b.

3 OBSERVATIONS

Our photometric observations in R filter were carried out with the Rozhen 2-m telescope with mean photometric precision of 0.002 mag. HAT-P-40 was observed on 2019 Oct 10 with 15 s exposures. HAT-P-51 was targeted on 2018 Nov 2 with 35 s exposures.

The standard procedure was utilized for calibration of the images (de-biasing and flat-fielding) by the software MAXIMDL. We tested several sets of reference stars (similar in brightness to or brighter than the targets) in order to obtain the most precise photometry. The R magnitudes (Table 3) of the chosen reference stars were obtained using their Sloan g and i magnitudes (APASS DR9, Henden et al. 2015) and the transformations of Jester et al. (2005). The photometry was performed by MAXIMDL and the obtained data were cleaned of trends (Figs. 1–2). The shape of the transit curve of HATP-40b seems slightly serrated. This is due to the atmospheric fluctuations during that night (notable for the small transit depth).

4 MODEL OF THE OBSERVED TRANSITS

Our photometric data were modeled via the code TAC MAKER 1.1.1 (Kjurkchieva et al. 2013, 2014). It does not use any simplifications of the configuration (dark planet, linear trajectory, etc.) and may fit data by linear, quadratic, square-root and logarithmic stellar LDL.

We fixed the values of stellar temperature $T_{\rm st}$, orbital radius a and initial epoch T_0 to the values from the previous solutions (Tables 1–2). The fitted parameters were the period P, stellar radius $R_{\rm st}$, planet radius R_p, orbital inclination *i*, planet temperature T_p and LDC. We varied these parameters around their values from the previous solutions (Tables 1–2) to search for the minimum of χ^2. It should be noted that we fitted the planet temperature T_p freely, instead of fixing it to T_{eq} values from the previous solutions.

We searched for transit solutions for different LDLs: linear, quadratic, square-root and logarithmic.

The results of our best transit solutions are expressed in the last columns of Tables 1–2. The synthetic curves are displayed in Figures 1–2 as continuous lines.

Considering the known values of masses M_p and $M_{\rm st}$ (Tables 1–2), we calculated the planet densities ρ_p and Safronov numbers Θ.

5 ANALYSIS OF THE RESULTS

5.1 HAT-P-40

We think our transit solution of HAT-P-40b is more accurate than that of Hartman et al. (2012) because it is based on more precise data as well as it is a result of reproducing a complete transit curve as opposed to the partial transits fitted by the discoverers. The new observations led to improving the orbital period of HAT-P-40 (Table 1).

The derived stellar radius from the transit solution is bigger by 2% than that determined by Hartman et al. (2012) from stellar models (Table 1).

The obtained planet radius of 1.676 R_J is bigger than the value of 1.62 R_J calculated by the empirical relation of Enoch et al. (2012) for a Jupiter-mass planet. Thus, the solution of the newly-observed transit confirms the conclusion of Hartman et al. (2012) that HAT-P-40b belongs to the family of highly inflated Jupiters with $0.4M_J < M < 1.5\,M_J$ and $R > 1.5\,R_J$.

The varying of T_p in the range 1000–2600 K led to changing of χ^2 by only 0.0007%. This means that the quality of our data does not allow determination of the planet temperature within this range.

The χ^2 values of the obtained best solutions for several LDLs differed by around 2%. The absolute minimum of χ^2 corresponded to the quadratic LDL (Table 1).

We found essential sensibility of the solution quality in terms of the LDC. It confirms the conclusion of Espinoza & Jordán (2015) that the fitting of the LDC in the transit-solution procedure leads to better results than fixing them to theoretical values. In the case of HAT-P-40, the fitted LDC for quadratic LDL u_1 = 0.310 and u_2 = 0.363 (Table 1) turned out close to the theoretical values u_1 = 0.329 and u_2 = 0.294 for filter R (Claret et al. 1995).

The precise astrometric *Gaia* distance of HAT-P-40 of 464.5 pc (Bailer-Jones et al. 2018) is smaller by around 7% than the calculated value by Hartman et al. (2012) based on the star luminosity obtained from the stellar models (Table 1). This means that probably the luminosity of HAT-P-40 estimated by the stellar models is bigger than the true value by the corresponding amount.

5.2 HAT-P-51

Our transit solution should be more accurate than that of Hartman et al. (2015) because it is based on more precise photometric data. The new observations led to improving the orbital period of HAT-P-51 (Table 1).

The stellar radius derived from our transit solution is bigger by 5% than that determined by Hartman et al. (2015) from stellar models (Table 2).

The planet radius of 1.414 R_J obtained from our transit solution is considerably bigger than the value of 0.923 R_J calculated by the empirical relation of Enoch et al. (2012) for a Saturn-mass planet.

The varying of the planet temperature T_p in the range 200–1600 K led to changing of χ^2 by only 0.01%. This means that the quality of our data does not allow precise determination of the planet temperature within this range.

The χ^2 values of the obtained best solutions for different LDLs differed by around 2%. The absolute minimum of χ^2 corresponded to the quadratic LDL of HAT-P-51. The fitted LDC for a quadratic LDL u_1 = 0.24 and u_2 = 0.28 (Table 2) turned out a little different from the theoretical values u_1 = 0.423 and u_2 = 0.242 for filter R (Claret et al. 1995).

Table 3 Coordinates and R Magnitudes of the Comparison Stars

Target	Comparison stars	RA (2000)	DEC (2000)	R
HAT-P-40	2MASS J01273318+3855375	01 27 33.2	+38 55 37.6	14.34
	2MASS J01275452+3854127	01 27 54.5	+38 54 12.7	13.98
HAT-P-51	TYC 2296–996–1	01 24 10.6	+32 47 23.9	12.34
	SDSS J012418.72+324925.2	01 24 18.8	+32 49 25.4	15.29

The *Gaia* distance of HAT-P-51 of 440 pc (Bailer-Jones et al. 2018) is smaller by around 6% than the calculated value by Hartman et al. (2015) based on the star luminosity obtained from the stellar models (Table 2). This means that the luminosity of HAT-P-51 estimated by the stellar models is bigger than the true value.

6 CONCLUSIONS

We presented new high-quality transit observations of the exoplanets HAT-P-40b and HAT-P-51b. Their modeling led to the following results.

(1) The orbital periods of the two targets were improved.

(2) The stellar radii derived from our transit solutions are bigger than those calculated from the stellar models by Hartman et al. (2012, 2015).

(3) The planet radii of HAT-P-40b and HAT-P-51b obtained from our transit solutions are bigger than the values calculated by the empirical relations of Enoch et al. (2012) for Jupiter-mass and Saturn-mass planets respectively. This confirms the highly-inflated nature of the two targets, especially for HAT-P-51b.

(4) The best transit solutions correspond to a quadratic LDL. We found that the fitted LDC of HAT-P-40 are close to the theoretical ones whereas those of HAT-P-51 are a little different. This means that the models of stellar atmospheres applied for estimation of LDC give quite reliable results taking into account the high sensitivity of the transit solution quality for the LDC.

(5) The *Gaia* distances of the two targets are smaller by 6–7% than the calculated values from the stellar models. This implies that the true stellar luminosities (and radii) of HAT-P-40 and HAT-P-51 are smaller than those determined from the stellar models. Hence, the stellar models and corresponding global stellar parameters would be improved on the basis of the *Gaia* distances. Moreover, this would allow more reliable determination of the parameters of the known exoplanets.

Acknowledgements The research was supported partly by project DN08/20 of Scientific Foundation of the Bulgarian Ministry of Education and Science, project D01-277/16.12.2019 of the Bulgarian Ministry of Education and Science and project RD RD-08-116/2020 of Shumen University. The authors are very grateful to the anonymous referee for the valuable comments.

This work has made use of data from the European Space Agency (ESA) mission *Gaia*, processed by the Gaia Data Processing and Analysis Consortium (DPAC). Funding for the DPAC has been provided by national institutions, in particular the institutions participating in the Gaia Multilateral Agreement. This research also has made use of the SIMBAD database, operated at CDS, Strasbourg, France, and NASA Astrophysics Data System Abstract Service.

References

Bailer-Jones, C. A. L., Rybizki, J., Fouesneau, M., et al. 2018, AJ, 156, 58
Claret, A., Diaz-Cordoves, J., & Gimenez, A. 1995, A&AS, 114, 247
Enoch, B., Cameron, A. C., Anderson, D. R., et al. 2011, MNRAS, 410, 1631
Enoch, B., Collier Cameron, A., & Horne, K. 2012, A&A, 540, A99
Espinoza, N., & Jordán, A. 2015, MNRAS, 450, 1879
Goldreich, P., & Soter, S. 1966, Icarus, 5, 375
Guillot, T. 2005, Annual Review of Earth and Planetary Sciences, 33, 493
Hartman, J. D., Bakos, G. Á., Béky, B., et al. 2012, AJ, 144, 139
Hartman, J. D., Bhatti, W., Bakos, G. Á., et al. 2015, AJ, 150, 168
Hebb, L., Collier-Cameron, A., Loeillet, B., et al. 2009, ApJ, 693, 1920
Henden, A. A., Levine, S., Terrell, D., et al. 2015, in American Astronomical Society Meeting Abstracts, 225, 336.16
Jester, S., Schneider, D. P., Richards, G. T., et al. 2005, AJ, 130, 873
Kjurkchieva, D., Dimitrov, D., Vladev, A., et al. 2013, MNRAS, 431, 3654
Kjurkchieva, D., Dimitrov, D., & Vladev, A. 2014, Bulgarian Astronomical Journal, 21, 85
Latham, D. W., Borucki, W. J., Koch, D. G., et al. 2010, ApJL, 713, L140
Mandel, K., & Agol, E. 2002, ApJL, 580, L171
Mandushev, G., O'Donovan, F. T., Charbonneau, D., et al. 2007, ApJL, 667, L195
Mazeh, T. 2008, in EAS Publications Series, 29, eds. M. J. Goupil & J. P. Zahn, 1
Pont, F., Husnoo, N., Mazeh, T., et al. 2011, MNRAS, 414, 1278
Smalley, B., Anderson, D. R., Collier-Cameron, A., et al. 2012, A&A, 547, A61